

PCCP

Accepted Manuscript



This is an *Accepted Manuscript*, which has been through the Royal Society of Chemistry peer review process and has been accepted for publication.

Accepted Manuscripts are published online shortly after acceptance, before technical editing, formatting and proof reading. Using this free service, authors can make their results available to the community, in citable form, before we publish the edited article. We will replace this *Accepted Manuscript* with the edited and formatted *Advance Article* as soon as it is available.

You can find more information about *Accepted Manuscripts* in the [Information for Authors](#).

Please note that technical editing may introduce minor changes to the text and/or graphics, which may alter content. The journal's standard [Terms & Conditions](#) and the [Ethical guidelines](#) still apply. In no event shall the Royal Society of Chemistry be held responsible for any errors or omissions in this *Accepted Manuscript* or any consequences arising from the use of any information it contains.

Nitrogen-doped carbon supports with terminated hydrogen and their effects on active gold species: A density functional study

Junjie Gu, Qian Du, You Han, Zhenghua He, Wei Li and Jinli Zhang*

School of Chemical Engineering and Technology, Tianjin University, Tianjin 300072,
P. R. China

Dr. Jinli Zhang

Professor of Chemical Engineering

School of Chemical Engineering & Technology

Tianjin University, Tianjin 300072, China

TEL: 86-22-27890643

FAX: 86-22-27890643

E-mail: zhangjinli@tju.edu.cn

Abstract

In order to disclose the reason that the N-doped carbon support can enhance the stability of Au-based catalysts for acetylene hydrochlorination, we established a big graphene cluster model of $C_{110}H_{28}$ to investigate the effect of different nitrogen-doped carbon supports on three kinds of gold species models of Au dimer, Au_2Cl_2 and Au_2Cl_6 through DFT calculations. Comparing the adsorption energy of each Au complex and the transferred charge from the support to Au complex, it is indicated that on the N-doped support GRN-I (the pyridinic N-doped graphene) the adsorption energies of Au dimer, Au_2Cl_2 and Au_2Cl_6 are greatly higher than those on other three kinds of supports, and Au complex accept most amount of transferred charges from the support of GRN-I. The effect of different supports on the adsorption of C_2H_2 and HCl was studied on Au_2Cl_6 /supports, suggesting that the co-adsorption of both reactants occurs on Au_2Cl_6 /GRN-I. The results indicate that the N-doped support of GRN-I can stabilize the gold species Au_2Cl_6 and enhance the interaction between Au_2Cl_6 and HCl, which can inhibit the reduction of Au^{3+} and then increase the long-term stability of Au-based catalysts.

Keywords: Au-based catalyst, density functional theory, nitrogen-doped carbon, graphene, acetylene hydrochlorination

1. Introduction

Acetylene hydrochlorination is one of the important reactions to produce vinyl chloride, which is the monomer to manufacture the popular engineering plastics polyvinyl chloride. At present, the main active component of current industrial catalysts is mercuric chloride, which is toxic and can result in serious environmental pollutions owing to its sublimation^{1,2}. Therefore, it has attracted lots of attentions to explore efficient non-mercuric catalysts for acetylene hydrochlorination³⁻⁹. Au-based catalysts on the carbon support have been intensively studied as a promising non-mercury catalyst for acetylene hydrochlorination. However, it is still a challenge to enhance the catalytic activity as well as the long-term stability of Au-based catalysts.

In order to improve the catalytic activity of gold catalysts, the effects of metallic additives, involving Pd, Cu,¹⁰ Ir,¹¹ La,¹² Co,^{6,13} etc have been studied on the Au-based catalysts. On the other hand, the effects of non-metallic dopants in the carbon support have also been studied on the catalytic performance of Au-based catalysts. For example, Wang et al. reported that phosphorus-doped carbon can enhance both the acetylene conversion and the selectivity to vinyl chloride over Au-based catalysts.¹⁴ Additionally Li et al prepared Au-based catalysts using nitrogen-doped (N-doped) carbon nanotubes as the support, and obtained an enhanced stability for acetylene hydrochlorination¹⁵, suggesting an important role of N-doped carbon support in augment of catalytic performance of Au-based catalysts. However, the mechanism that N dopants of the carbon support can enhance the catalytic stability of Au-based

catalysts is elusive yet.

Graphene has been considered as a promising carbon support for catalysts, owing to its unique molecular structure and physicochemical properties, high electrical conductivity and large specific surface area.¹⁶⁻¹⁸ Recently, the nitrogen-doped graphene, involving different N-doped bonding configurations of the graphitic N, the pyridinic N and the pyrrolic N,¹⁹ have been reported to improve the performance of certain catalysts for the oxygen reduction,²⁰⁻²³ hydrogen peroxide reduction reaction²⁴ or other reactions.²⁵ Moreover, Density-Functional Theory (DFT) calculations have been used to study the effect of N dopants on the related reaction at the electronic level. For instance, Groves et al. used DFT to explain the strength of the Pt on nitrogen-doped graphene surface.²⁶ Zhang et al.^{27, 28} calculated the reaction path of ORR on nitrogen-doped graphene. In addition, Akola and Häkkinen²⁹ established a slab model with C144 atoms in a supercell to study the adsorption energies of Au atom on the graphene. These results enlightened us to select N-doped graphene as the model of carbon support to investigate the influence of N dopants on the active gold species of Au-based catalysts via DFT calculations.

Previously, DFT calculations³⁰ suggested that the reduction of Au³⁺ could be one probable deactivation reason for the gold catalysts during the acetylene hydrochlorination reaction. Three typical gold species including Au³⁺, Au⁺ and Au⁰ have been reported in the Au-based catalysts with the carbon support.^{6, 14, 31} In this article, a big graphene cluster model including C110 atoms and terminated hydrogen atoms was built to investigate the effect of different nitrogen-doped carbon supports

on the catalytic stability of gold catalysts for acetylene hydrochlorination, including three kinds of gold species models of Au dimer, Au_2Cl_2 and Au_2Cl_6 . Comparing the adsorption energy of each gold species as well as the charge transfer from the N-doped support, it was indicated that the active gold species of Au_2Cl_6 were most stabilized on the pyridinic N-doped graphene. Further the co-adsorption configurations of both reactants, acetylene and hydrogen chloride, were studied on Au_2Cl_6 with the pyridinic N-doped support so as to disclose the reason that the N-doped carbon support can enhance the stability of Au-based catalysts. This work provided a useful guidance on modulating the stability of active gold species via the N-doped carbon support for Au-based catalysts of acetylene hydrochlorination.

2. Calculation method and models

All the calculations were carried out using DFT as theoretical basis by Dmol³ code of Materials Studio software from Accelrys Inc. A spin-polarized revised Perdew-Burke-Ernzerhof (RPBE)^{32, 33} functional within the formulation of the generalized gradient approximation (GGA) was employed to handle the exchange and correlations. The spin multiplicity was selected as doublet for Au atom and singlet for Au dimer. The DNP basis set and the All Electron Relativistic core treatment were used in all of the calculations^{34, 35}. The energy convergence criteria was set as 0.0005 eV, and the atomic structures were relaxed until the forces on all unconstrained atoms were less than $0.109 \text{ eV}\cdot\text{\AA}^{-1}$. A smearing of 0.136 eV to the orbital occupation was applied to achieve the self-consistent field convergence.

In order to analyze the stability of Au-based catalyst with different valence states

on the pristine and N-doped graphene, the adsorption energy was defined as equation (1).

$$E_{\text{ads}} = -(E_{\text{total}} - E_{\text{Au}} - E_{\text{support}}) \quad (1)$$

where E_{total} is the energy of the optimized structure of adsorption complex, E_{Au} and E_{support} are the total energies of the free adsorbate and the bare support after geometry optimization, respectively.

After the geometry optimization, there appears somewhat deformation of the adsorption complex. Thus, the adsorption energy was classified into two parts: one was the interaction energy and the other was the deformation energy, which are defined by equations (2) and (3) respectively.

$$E_{\text{inter}} = -(E_{\text{total}} - E_{\text{Au-a}} - E_{\text{support-a}}) \quad (2)$$

$$E_{\text{defor}} = E_{\text{ads}} - E_{\text{inter}} = -\left[(E_{\text{Au-a}} - E_{\text{Au}}) + (E_{\text{support-a}} - E_{\text{support}})\right] \quad (3)$$

where $E_{\text{Au-a}}$ and $E_{\text{support-a}}$ are respectively the single point energy of the adsorbate and support, of which the structure comes from the optimized geometry of the adsorbed system.

The adsorption energy of HCl or C₂H₂ was calculated by equation (4).

$$E_{\text{ads}}(\text{reactant}) = -(E_{\text{total}} - E_{\text{Au}_2\text{Cl}_6/\text{support}} - E_{\text{reactant}}) \quad (4)$$

where $E_{\text{Au}_2\text{Cl}_6/\text{support}}$ indicates the energy of the Au₂Cl₆ adsorbed on the support, and E_{reactant} is the total energy of HCl or C₂H₂ after geometry optimization.

The doping energy, E_{doping} was calculated by equation (5) to estimate the probable location of the doped N atom in the graphene.

$$E_{\text{doping}} = E_{\text{GRN}} + E_{\text{C}} - E_{\text{graphene}} - E_{\text{N}} \quad (5)$$

where E_{GRN} and E_{graphene} are the total energy of graphene with and without N dopant, respectively. E_{C} and E_{N} are the total energy of a single C atom from graphite and N atom from the N_2 , respectively.

Electronic property analysis was carried out to understand the interaction between N-doped graphene and active gold species in Au-based catalysts. Mulliken charges and the deformation electron density that indicates the electron density difference of each atom before and after the adsorption of Au complex were adopted to investigate the charge transfer. Density of state (DOS) and partial density of states (PDOS) were used to measure the interaction of the catalysts and the supports.

A pristine graphene model was built containing 42 hexagonal rings ($\text{C}_{110}\text{H}_{28}$). It is a single layer graphene cluster. Its length was 17.965 Å, and the width was 17.892 Å. The C-C bonds in graphene are about 1.42 Å, which are in good agreement with experimental work³⁶ and calculation.³⁷ In order to make the label more pithily, graphene was abbreviated to GR. Based on this pristine graphene model, three typical structures of nitrogen doped graphene were constructed with the similar configuration (Figure 1), involving the pyridinic N ($\text{C}_{109}\text{NH}_{28}$) (abbreviated to GRN-I), pyrrolic N ($\text{C}_{110}\text{NH}_{27}$) (abbreviated to GRN-II) graphitic N ($\text{C}_{109}\text{NH}_{28}$) (abbreviated to GRN-III), respectively. Carbon or nitrogen atoms on the edge of the graphene were terminated by hydrogen atoms.

Au-based catalysts, prepared using the precursor of AuCl_3 and the carbon support, have been considered as one of the promising non-mercuric catalysts for acetylene hydrochlorination reaction. In our previous work, experimental results indicated that

there are three kinds of gold species in the Au-based catalysts for acetylene hydrochlorination, involving Au^{3+} , Au^+ and Au^0 .^{6,14} Therefore, we established three models for active gold species, including metallic gold, Au_2Cl_2 and Au_2Cl_6 , of which the stability is discussed in the section of 3.2, 3.3 and 3.4 respectively.

(Figure 1)

3. Results and discussion

3.1 Nitrogen-doped graphene supports

The geometrical structures of pristine and N-doped graphene were optimized before Au complex was adsorbed on the graphene support. As shown in Figure 2a'~2d', the length of the bonds connected with the doped nitrogen is changed, although the optimized geometry of the GRN-I, GRN- II and GRN- III are similar with that of the GR. In the GR, the bond lengths of C-C and C-H are 1.416 Å and 1.089 Å, respectively. For the N-doped graphene, the N-C bond is as short as 1.417~1.418 Å on GRN- III, the N-H bond is 1.014 Å on the GRN- I and 1.012 Å on the GRN- II. According to the Mulliken charges, indicated by the red color number in Figure 2a~2d, the negative charge tends to concentrate on N atom, which is more electronegative than C atom (The electronegativities of C is 2.55, and N atom is 3.04 according to Pauling scale). The Mulliken charge of N atom is -0.282 e for the GRN-I, -0.400 e for the GRN-II and -0.397 e for the GRN-III, respectively. While the H atom connected with N atom exhibits more positive charge than that connected with C atom. Especially the H atom connected with the pyridinic N displays the most positive charge of 0.193 e.

Mulliken bond order analysis can measure the covalent and metallic properties of the bond. In Dmol³, Mulliken bond order reflects the value of the sharing electrons in the middle of the bond. If the value of the Mulliken bond order is positively larger, the bond behavior is more covalent rather than metallic. The Mulliken bond order analysis indicates that the N-H bond order is respectively 0.777 for the GRN-I, 0.780 for the GRN-II, and 0.748 for C-N bond on the GRN-III, whereas the C-H bond order is 0.832 without N-doping. The results illustrate that the polarity of the N-H bond is stronger than that of C-H bond, the doped N atom has stronger interaction with C or H atom. Comparing the deformation electron density of different supports (Figure S1 in the supporting information), it is indicated that in the presence of N dopant the conjugated electrons on rings contained N atom are not as equality as usual, and the C-N bond is polarized, with more electrons concentrated on N atom.

(Figure 2)

The doping energy was calculated to estimate the probable location of a dopant N atom in the graphene. The E_{doping} value of the GRN-I, GRN-II and GRN-III is 1.46, 0.45 and 1.94 eV, respectively. The changing order of the doping energy is GRN-II < GRN-I < GRN-III. The larger the doping energy value, the more difficult the N-doped graphene is formed. Therefore, the GRN-II and GRN-I are preferentially generated, which is consistent with the previous experimental report³⁸. In the case of GRN-III, it requires to break three C-C bonds to dope the graphitic N, consequently the N doping in the middle of the graphene is more difficult than that at the edge site.

DOS plots display that for the pristine graphene the DOS is continuous near the

Fermi level and distributed in both sides of Fermi level at 0 eV, owing to the excellent electronic conductivity. For the nitrogen-doped graphene supports, as shown in Figure S2, there is no obvious change near the Fermi level, but a new DOS peak appears at -22.0 eV for the GRN-I, at -20.5 eV for the GRN-II and at -22.5 eV for the GRN-III, respectively. It is clear that the new peak attributes to the N dopant, which causes the variation of electronic properties of the graphene so as to generate a new DOS structures. In addition, PDOS plots of GR and GRN-I, as shown in Figure S3, indicate that the new peak around -22.0 eV is mainly attributed to the *s* orbitals of N atom as well as the *s* and *p* orbitals of H atom that is bonded with N.

3.2 Au atom and Au dimer on the pristine and N-doped graphene

In order to study the effect of N-doped support on the stability of active metallic gold catalytic species for acetylene hydrochlorination, the Au atom and Au dimer models were established on different supports including the GR, the GRN-I, GRN-II and GRN-III, based on previous literatures about nano metallic materials³⁹⁻⁴¹. At first, the single Au atom is initially set at the hole site of the hexagonal ring of graphene, after optimization, as shown in Figure 3a, the adsorbed Au atom on the GR is located at the bridge site of two neighboring H atoms at the edge of the support, with the distance between Au atom and each H atom is respectively 2.824 and 3.055 Å. Similarly, the adsorbed Au atom on the GRN-I is located at the bridge site of two neighboring H atoms, one of which is connected with the N dopant. And the distance between Au atom and each H atom is respectively shorten to 2.611 and 2.637 Å (Figure 3b). On the GRN-II, the adsorbed Au atom interacts with only one H atom

that is connected with the N dopant, owing to the large gap between two neighbored H atoms. And the Au-H interacting distance is 2.335 Å (Figure 3c). While on the GRN- III with no active H atoms connected with the N dopant, the adsorbed Au atom is located on the top site of N dopant (Figure 3d). The E_{ads} of Au atom on these supports decreases in the order of: GRN- I (5.86 eV) > GRN- II (5.46 eV) > GR (5.35 eV) > GRN- III (5.20 eV), illustrating that the GRN-I and GRN-II are beneficial to augment the adsorption stability of Au atom. Previously Varns and Strange built a C32 atoms graphene sheet supercell and the calculated E_{ads} of Au atoms was 0.79 eV³⁹. Whereas adopting our model of C110 graphene cluster, the E_{ads} of Au atoms is calculated as 5.35 eV. The value difference of E_{ads} is mainly caused by different models and calculation methods. For example, Groves et al has reported that the structure models and calculation methods can greatly affect the value of the binding energies, however, no matter which models and calculation methods were used it can reflect the similar variation tendency of metal adsorption on the N dopant surface²⁶.

In addition, the deformation energy was calculated to assess the deformation of different supports caused by the adsorbed Au atom, as shown in Figure 3, the E_{defor} values on four kinds of supports are close to zero. It is confirmed that the difference of adsorption energies of Au atom on these supports is mainly attributed to the individual interaction between Au and different support.

(Figure 3)

Before adsorption, the Au atom was zero valence state. After adsorption, there occur the interactions between Au and H atoms, as shown in Figure 3, the closest

bond distance of Au-H is 2.824 Å on GR, 2.611 Å on GRN-I, 2.335 Å on GRN-II respectively. And the transferred charge to Au atom is respectively 0.259 e, 0.439 e, 0.323 e and 0.284 e from the support of GR, GRN-I, GRN-II and GRN-III. It is indicated that the interaction between Au atom and H atom in the support greatly affects the charge of Au atom.

In order to disclose the reason that results in the difference of adsorption stability of Au atom on four kinds of supports, the deformation electron density of adsorbed Au atom on the GR, GRN-I, GRN-II and GRN-III are displayed in Figure 4. It is illustrated that the blue and purple shadows around Au atom adsorbed on GRN-III are not discernable, comparing with that adsorbed on GRN-I and GRN-II. Therefore the charge transfer from GRN-III to Au atom is negligible. In addition, the amount of transferred electrons from the GRN-I to Au is larger than that from the GRN-II. In combination with the adsorption energy, it is indicated that the more transferred electrons from the support to Au atom, the more stable adsorption of Au atom occurs.

(Figure 4)

For the optimized Au dimer model, the Au-Au bond is stretched to some extent, with the bond length equal respectively 2.524 Å on the GR, 2.552 Å on the GRN-I, 2.528 Å on the GRN-II and 2.520 Å on the GRN-III (Figure 5), while in gas phase the Au-Au bond length is 2.508 Å. In the most stable structure on the GR, Au dimer is adsorbed parallel with the edge of the support, with the distance between each Au atom and the nearest H atom ranged from 3.300 to 3.774 Å, a little longer than those in the corresponding adsorbed Au atom model. For Au dimer adsorbed on the GRN-I,

the closest distance between each Au atom and related H atom is 2.408 and 2.726 Å. On the GRN-II, the Au-Au bond is initially parallel with the N-H bond, while after the geometry optimization the Au-Au bond turns to be perpendicular to the planar GRN-II, with the distance between Au and H equal 2.691 Å. In the optimized structure of the GRN-III, the adsorbed Au-Au bond is parallel to the N-C bond, and the distance between Au and N atom is 4.152 Å, suggesting that the interaction between Au dimer and graphitic N is relatively weak so as to result in a smaller stretching of Au-Au bond, comparing with Au dimer adsorbed on other three kinds of supports. The E_{ads} of Au dimer on these supports decreases in the order of: the GRN-I (5.77 eV) > GRN-II (5.43 eV) > GR (5.36 eV) > GRN-III (5.20 eV), similar with the order of the Au atom model. Through charge distribution analysis in Table S1, it is indicated that Au atoms can easily obtain electrons from the supports, especially on the GRN-I the adsorbed Au dimer can obtain much more electrons. According to the electron properties of different N-doped graphene, as discussed in section 3.1, the N-H bond of GRN-I (pyridinic N-doped) support is most similar to metallic bond, comparing the GRN-II and GRN-III. After Au dimer adsorption, the charge transfer to Au dimer is 0.333 from the support of GRN-I, 0.188 from GRN-II and 0.135 from GR-III. The more transferred charge to Au dimer from the GRN-I is attributed to the metallic bond of N-H of GRN-I.

(Figure 5)

These results suggest that the N-doped support can enhance the adsorption energy of Au atom and Au dimer. Previously, Akola and Häkkinen²⁹ established a slab model

with C144 atoms in a supercell, adopting GGA-PBE in CPMD, to study the adsorption energies of Au atom on the graphene. Their calculations also indicated that the adsorptions of Au atom on the N-doped graphene were more stable than those on the graphene, and more negative charges were transferred to the adsorbates from the N doped graphene, although the values of the adsorption energies and the transferred charges were different from our work owing to the different model and calculation method used.

The PDOS analysis for the adsorbed Au dimer on different graphene supports is shown in Figure S4. After Au dimer is adsorbed on graphene, a new peak of *s* orbital from H atom appears at about -2.0 eV, which is hybridized with the *d* orbitals of Au atoms. On the GRN-I, there also appears a new peak of *s* orbital from H atom at about -2.0 eV, which is hybridized with *d* orbitals of Au atoms. These results suggest that the H atom has significant interactions with Au dimer.

3.3 Au₂Cl₂ on the pristine and N-doped graphene

Two typical structures of Au₂Cl₂, involving the triangular model and the tetragonal model, were constructed and optimized, according to the typical tetragonal crystal structure of AuCl⁴². As shown in the top panel of Figure 6, the Au and Cl atoms are numbered orderly. The triangular model of Au₂Cl₂ is comprised of a triangle including atoms Au1, Au2 and Cl2, as well as the atom Cl1 connected Au1 with the bond length of 2.282 Å. While the tetragonal model consists of two triangles, each of them including two Au atoms and one Cl atom. The total energy of triangular model is about 0.82 eV lower than the tetragonal model, suggesting that the triangular

model is the more stable configuration.

Au_2Cl_2 adopting the triangular model was chosen to study the adsorption on four different graphene supports. Both Au and Cl atoms can interact with H atom, thus, the Au_2Cl_2 was initially laid at the edge of the support, with the line of Cl1-Au1-Cl2 parallel to the edge of the GR, GRN-I and GRN-II. While in the case of the GRN-III the planar triangle of Au_2Cl_2 was set parallelly on the top of the N atom. As shown in Figure 6, being adsorbed on the GR, the structure of Au_2Cl_2 shows no obvious deformation, the bond length of Au2-Cl2 is increased from the original 2.413 Å to 2.702 Å, while the bond length of Au1-Au2 has no change at 2.664 Å. When adsorbed on the GRN-I, the structure of Au_2Cl_2 is greatly deformed into a “T” type structure, owing to the bond breaking of Au2-Cl2. The total energy of “T” type is 0.02 eV, higher than that of the triangular Au_2Cl_2 , suggesting that the “T” type Au_2Cl_2 is not so stable as the triangular one. The bond length of Au1-Au2 decreases from the original 2.664 Å to 2.623 Å, and the angle of Au2-Au1-Cl2 changes from the original 56.7° to 94.0°. The shortest distance between Cl atom and H atom in the GRN-I is 2.512 Å. The N doping can enhance the interaction between H atom of the support and Cl atom of Au_2Cl_2 . Thus the angle Au2-Au1-Cl2 becomes larger than the initial. In addition, the Au1-H bond is also shortened from 3.395 Å on GR to 3.031 Å on GRN-I.

When being adsorbed on the GRN-II, the Au_2Cl_2 maintains the triangular structure but with a little deformation, the bond length of Au2-Cl2 is stretched up to 2.922 Å, and the angle of Au2-Au1-Cl2 changes from the original 56.7° to 73.0°. The shortest distance between Cl atom and H atom of GRN-II is 3.383 Å, approximate to

3.402 Å of GR.

In the case of the GRN-III, the adsorbed Au₂Cl₂ also deforms into the “T” type structure, with the Au1-Au2 bond length of 2.623 Å, the Au2-Au1-Cl2 angle of 94.0°. The E_{ads} of Au₂Cl₂ on these supports decreases in the order of: GRN-I (6.20 eV) > GRN-II (5.70eV) > GR (5.66eV) > GRN-III (5.57eV), illustrating that the adsorption of Au₂Cl₂ is the most stable on the GRN-I, whereas on the GRN-III the adsorption of Au₂Cl₂ is less stable than that on the GR.

Table 1 lists the charge distribution of Au₂Cl₂ adsorbed on different supports. The total charge of two Au atoms is 0.36 e in a vacuum, with Au1 atom of 0.102 e and Au2 atom of 0.258 e, and the total charge of two Cl atoms is -0.36 e. After Au₂Cl₂ adsorption, the two Cl atoms of Au₂Cl₂ accept more transferred charges from the support including GR, GRN-1, GRN-II, and GRN-III, while the two Au atoms have less positive charges on these four supports. For the support of GR before adsorption of Au₂Cl₂, as shown in Figure S6 in the supporting information, the four C atoms at the edge of GR have the charge around -0.075 e ~ -0.065 e, and the terminated H atoms have the charge around 0.034 e ~ 0.044 e; while after adsorption of Au₂Cl₂, the charges of four C atoms at the edge change to be around -0.088 e ~ -0.106 e, and the charges of terminated H atoms change to be around 0.102 e ~ 0.129 e. In the case of the support of GRN-I before the adsorption of Au₂Cl₂ (Figure S7 in the supporting information), the N atom at the edge has the charge of -0.282 e and the C atom connected with N atom has the charge of 0.053 e, the other two C atoms at the edge have the charge of -0.097 e and -0.059 e, and the terminated H atoms have the charge

around 0.102 e ~ 0.129 e. After adsorption of Au₂Cl₂, the charge of N atom of GRN-I changes to be -0.309 e and the charge of C atom connected with N atom changes to be 0.069 e, the charges of other two C atoms at the edge of GRN-I change to be -0.086 e and -0.129 e, and the positive charges of terminated H atoms increase to 0.112 e ~ 0.278 e. Therefore, it is indicated that the charges of N atom, C atoms and the terminated H atoms at the edge of the support change greatly before and after adsorption of Au₂Cl₂, and the terminated H atoms are important to accomplish charge transfers from the support to Au₂Cl₂.

(Figure 6)

(Table 1)

3.4 Au₂Cl₆ on the pristine and N-doped graphene

Au₂Cl₆ was chosen as the model of Au³⁺ species, according to the previous work suggesting that AuCl₃ tends to form the planar Au₂Cl₆ dimer in the gas phase³⁰. Au₂Cl₆ was initially laid on the flat surface of graphene to maximize its interaction with the support. However, after geometry optimization Au₂Cl₆ tilts to interact with terminated H atoms at the edge of the GR, GRN-I- and GRN- II (shown in Figure 7). The $E_{\text{ads}}(\text{Au}_2\text{Cl}_6)$ decreases in the order: GRN- I (6.36 eV) > GRN-III (6.05 eV) > GRN-II (6.03 eV) > GR (5.91 eV), indicating that in the presence of N dopant the interaction between Au₂Cl₆ and the support is enhanced, with the strongest interaction occurred in the GRN- I.

As shown in Figure 7, the bond length between the second Au atom and the sixth chlorine atom in Au₂Cl₆ complex, i.e., Au₂-Cl₆ bond length, is 2.264 Å in the gas

phase. After being adsorbed on the support of GR, GRN- I, GRN- II and GRN- III, the Au₂-Cl₆ bond length increases to 2.308, 2.370, 2.333 and 2.318 Å, respectively. It is suggested that the Au₂-Cl₆ bond becomes weakened owing to the interfacial interaction. The distance between Cl₆ and the nearest H atom is 2.425, 2.750 and 4.207 Å for the GRN-I, GRN-II and GR, suggesting that H atoms of the support GRN-I and GRN-II play an important role in stabilizing the adsorption of Au₂Cl₆. This is consistent with previous reports showing that the edge or defect of graphene could provide more active sites.^{42, 44}

(Figure 7)

Table 2 lists the charge distribution of Au₂Cl₆ adsorbed on different supports. In the case of single Au₂Cl₆ in gas phase, the total charge of two Au atoms is 0.264 e, and the total charge of six Cl atoms is -0.264 e. For Au₂Cl₆ adsorbed on the GR, the charge of Au and Cl atoms changes to 0.265 e and -0.891 e respectively. The total charge of two Au atoms shows only small variation on different support. However, the total charge of six Cl atoms changes obviously, equal to -0.891, -1.158, -0.986, and -1.053 respectively on the support of GR, GRN-I, GRN-II and GRN-III. Especially the individual charge of the sixth Cl atom (Cl₆) is greatly affected by the N-doped support, equal to -0.227 on GR, -0.331 on GRN-I, -0.271 on GRN-II and -0.261 on GRN-III respectively. It is indicated that the charges from the N-doped graphene supports are transferred mainly to Cl atoms in Au₂Cl₆ complex. The net charge of the N-doped support with adsorbed Au₂Cl₆ is negative, with the total charge value increasing in the order of GRN-I (-0.888 e) > GRN-III (-0.794 e) > GRN-II

(-0.713 e) > GR (-0.626 e). In addition, the bond order of Au₂-Cl₆ is 0.505 for the Au₂Cl₆ in gas phase, while it decreases to 0.471 for Au₂Cl₆ adsorbed on the GR. In the case of Au₂Cl₆ adsorbed on the N-doped graphene, the bond order of Au₂-Cl₆ decreases to 0.459 for the GRN-III, 0.450 for the GRN-II, and 0.415 for the GRN-I respectively. It is indicated that in the presence of N-doped support the adsorbed Au₂Cl₆ exhibits higher degree of polarization, comparing with that on the GR.

(Table 2)

The interaction between Au₂Cl₆ and H atoms in the GRN-I was further studied against that in the GR. As shown in Figure 8, after the adsorption of Au₂Cl₆, there is a new peak near 2 eV, which belongs to the *s* orbital of H atoms (denoted with the blue arrows), which is hybridized with the *p* orbital peak of Cl atoms in Au₂Cl₆. On the contrary, the PDOS profiles of H atoms in the GR show no significant variation before and after the adsorption of Au₂Cl₆, without any coincident peak of Cl atoms in Au₂Cl₆. It is confirmed that H atoms in the GRN-I interact significantly with Cl atoms in Au₂Cl₆.

(Figure 8)

3.5 Gold species on N-doped supports: the stability and its adsorption towards reactants

Based on the above three typical models involving Au dimer, Au₂Cl₂ and Au₂Cl₆, we compared the adsorption energy of each gold species on different supports including the GR, GRN-I, GRN-II and GRN-III as well as the transfer electrons from the support to Au complex. As shown in Figure 9, on the GR Au₂Cl₆ shows the largest E_{ads} (5.91 eV), Au dimer is the lowest (5.36 eV), with Au₂Cl₂ as the intermediate (5.66

eV), suggesting the most stable adsorption of Au_2Cl_6 . In the case of N-doped supports, the preferential adsorbed order of gold species is as same as that on the GR. It deserves to mention that on the support GRN-I the adsorption energies of Au dimer, Au_2Cl_2 and Au_2Cl_6 are greatly higher than those on other three kinds of supports, with the largest E_{ads} value (6.36 eV) achieved for Au_2Cl_6 , followed by 6.20 eV for Au_2Cl_2 and 5.77 eV for Au_2 . On the other hand, as shown in Figure 10, the Mulliken charge analysis indicates that the transferred charge (Δq) from different support to Au dimer, Au_2Cl_2 and Au_2Cl_6 rises in the order of Au dimer < Au_2Cl_2 < Au_2Cl_6 . For instances, on the support of GR, the transferred charge to Au complex is in the order of Au dimer (0.138 e) < Au_2Cl_2 (0.358 e) < Au_2Cl_6 (0.626 e); while on the N-doped support GRN-I, the transferred charge to Au complex is Au dimer (0.333 e) < Au_2Cl_2 (0.563 e) < Au_2Cl_6 (0.888 e). Therefore, the most stabilized gold species of Au_2Cl_6 is selected to study further the effect of different supports on the adsorption of C_2H_2 and HCl, two reactants in the acetylene hydrochlorination reaction.

(Figure 9)

(Figure 10)

Figure 11 displays the optimized structures for HCl adsorbed on Au_2Cl_6 /supports, with the initial position of HCl located at the bridge site between Cl3 and Cl6 atoms of Au_2Cl_6 (Figure S8 in the supporting information). After the geometry optimization, on Au_2Cl_6 /GR the adsorbed HCl is located in the middle of two Cl atoms of AuCl_3 , with the distance between H atom of HCl and Cl3 atom of Au_2Cl_6 equals to 2.487 Å and that between H(HCl) and Cl6 atom is 3.681 Å respectively, the bond length of Au2-Cl6 stretched from 2.308 Å (Figure 7a) to 2.313 Å (Figure 11a) and the bond

length of HCl increased from the original 1.286 Å to 1.302 Å. On the Au₂Cl₆/GRN-II, the stable adsorbed location of HCl is similar with that on GR, with the distances between H atom of HCl and Cl3 atom of Au₂Cl₆ equals 2.319 Å and that between H(HCl) and Cl6 atom is 3.610 Å, the bond length of Au2-Cl6 stretched from 2.333 Å (Figure 7c) to 2.346 Å (Figure 11c) and the bond length of HCl increased to 1.311 Å. In the presence of the adsorbed HCl, the Au₂Cl₆ plane is still parallel with the support of either GR or GRN-II, with the distance between the nearest H atom in the support and the Cl atom of Au₂Cl₆ equal 3.706 Å and 2.540 Å, respectively.

On the Au₂Cl₆/GRN-I, the stable adsorbed location of HCl is on the top of Cl atom of Au₂Cl₆, with the distance between H atom of HCl and Cl3 atom of Au₂Cl₆ equals 2.330 Å, the bond length of Au2-Cl6 stretched from 2.370 Å (Figure 7b) to 2.404 Å (Figure 11b) and the bond length of HCl increased to 1.307 Å, especially the distance between the nearest H atom in the support and Cl6 atom of Au₂Cl₆ is shortened from 2.425 Å (Figure 7b) to 2.194 Å (Figure 11b). Thus the Au₂Cl₆ plane is inclined to be unparallel with the support, owing to the strong interaction between the adsorbed HCl and Au₂Cl₆. On the Au₂Cl₆/GRN-III, the adsorbed HCl is located on the top of the Cl atom of Au₂Cl₆, with the distance between H atom of HCl and Cl atom of AuCl₃ equal 2.370 Å, the bond length of Au2-Cl6 stretched from 2.318 Å (Figure 7d) to 2.338 Å (Figure 11d) and the bond length of HCl increased to 1.306 Å. The $E_{\text{ads}}(\text{HCl})$ is respectively 0.41 eV, 0.39 eV, 0.48 eV, and 0.72 eV on the support of the GR, GRN-III, GRN-II and the GRN-I, reflecting the stabilized adsorption of HCl on Au₂Cl₆/GRN-I.

After adsorption on $\text{Au}_2\text{Cl}_6/\text{supports}$, the net charge of HCl is -0.035 on GR, -0.049 on GRN-I, -0.041 on GRN-II and -0.047 on GRN-III respectively, as listed in Table S2 in the supporting information; meanwhile, the net charge of Au_2Cl_6 donot change obviously, equal -0.665e, -0.886e, -0.736 e and -0.798 e respectively. It is indicated that the adsorbed HCl accepts the charge from the support.

(Figure 11)

Figure 12 shows the optimized structures for C_2H_2 adsorbed on $\text{Au}_2\text{Cl}_6/\text{supports}$, with the initial position of C_2H_2 similar with that of HCl. Before the adsorption, C_2H_2 has the C-H bond length of 1.071 Å and the C-C of 1.214 Å. On $\text{Au}_2\text{Cl}_6/\text{GR}$ and $\text{Au}_2\text{Cl}_6/\text{GRN-II}$, the nearest distance between H atom of the adsorbed C_2H_2 and Cl atom of Au_2Cl_6 is 3.036 Å and 2.801 Å respectively, and the adsorbed C_2H_2 exhibits the C-C bond length of 1.216 Å on both supports while the C-H bond length of 1.075 Å on GR and 1.077 Å on GRN-II. On $\text{Au}_2\text{Cl}_6/\text{GRN-I}$ and $\text{Au}_2\text{Cl}_6/\text{GRN-III}$, the nearest distance between H atom of the adsorbed C_2H_2 and Cl atom of Au_2Cl_6 is 2.976 Å and 2.690 Å, respectively, and the adsorbed C_2H_2 exhibits the stretched C-H bond length of 1.075 Å and the C-C bond length of 1.214 Å on the GRN-I, while on the GRN-III the C-H and C-C bond length of adsorbed C_2H_2 is increased to 1.075 Å and 1.216 Å, respectively. The $E_{\text{ads}}(\text{C}_2\text{H}_2)$ is respectively 0.42 eV, 0.35 eV, 0.46 eV, and 0.71 eV on the support of the GR, GRN-III, GRN-II and the GRN-I, suggesting the strongest adsorption of C_2H_2 on $\text{Au}_2\text{Cl}_6/\text{GRN-I}$.

(Figure 12)

Comparing Figure 11 with Figure 12, it is illustrated that the adsorption of C_2H_2 and HCl on Au_2Cl_6 is greatly associated with the site of N dopant in the support. It is

on the GRN-I that the adsorptions of both C_2H_2 and HCl are the strongest, with the adsorption energy of 0.71 eV and 0.72 eV respectively. As far as the approximate location site of individual reactant is considered, we further investigated the co-adsorption of both reactants on $Au_2Cl_6/GRN-I$, the initial positions of C_2H_2 and HCl (Figure S9 in the supporting information) are adopted according to our previous work³⁰. As shown in Figure 13, after geometry optimization, the structure of C_2H_2 is deformed, with the C-C bond length stretched from 1.214 Å to 1.279 Å, and the C-Au bond distance about 2.0 Å. The bond length of HCl is stretched from 1.295 Å to 1.328 Å, and the closest distance between H atom of HCl and Cl atom of Au_2Cl_6 is 2.166 Å. The $E_{ads}(co-adsorption)$ is 1.58 eV. Both adsorbed reactants are activated on $Au_2Cl_6/GRN-I$.

There are two main reaction paths for acetylene hydrochlorination over Au_2Cl_6 , reported in the previous work³⁰. The energy barriers of these two paths are 1.27 and 1.01 eV, respectively. Additionally there are two side reactions in the case of preferential adsorption of C_2H_2 , with the individual energy barrier of 1.29 and 1.04 eV respectively. Thus, there exist competitive reaction paths for acetylene hydrochlorination over Au-based catalysts, especially the preferential adsorption of C_2H_2 can cause the deactivation of active Au^{3+} species. Here the results indicate that the N-doped support of GRN-I can stabilize the gold species Au_2Cl_6 and enhance the interaction between Au_2Cl_6 and HCl, which can inhibit the lost of Cl atoms from Au_2Cl_6 and retard the reduction of Au^{3+} and then increase the long-term stability of Au-based catalysts. This work provides a useful guidance on modulating the stability

of active gold species via the N-doped carbon support for Au-based catalysts of acetylene hydrochlorination.

(Figure 13)

4. Conclusion:

A big graphene cluster model of $C_{110}H_{28}$ was built to investigate the effect of different nitrogen-doped carbon supports on the catalytic stability of gold catalysts for acetylene hydrochlorination, including three kinds of gold species models of Au dimer, Au_2Cl_2 and Au_2Cl_6 . Comparing the adsorption energy of each Au complex on different supports including the GR, GRN-I, GRN-II and GRN-III as well as the transfer electrons from the support to Au complex, it is indicated that on the N-doped support GRN-I (the pyridinic N-doped graphene) the adsorption energies of Au dimer, Au_2Cl_2 and Au_2Cl_6 are greatly higher than those on other three kinds of supports, with the largest E_{ads} value (6.36 eV) achieved for Au_2Cl_6 , followed by 6.20 eV for Au_2Cl_2 and 5.77 eV for Au dimer. The Mulliken charge analysis indicates that the transferred charge from different support to Au complex rises in the order of Au dimer < Au_2Cl_2 < Au_2Cl_6 .

Then the most stabilized gold species of Au_2Cl_6 is selected to study further the effect of different supports on the adsorption of C_2H_2 and HCl, two reactants in the acetylene hydrochlorination reaction. It is shown that the most stabilized adsorption of either HCl or C_2H_2 is on $Au_2Cl_6/GRN-I$, with $E_{ads}(HCl)$ of 0.72eV and $E_{ads}(C_2H_2)$ 0.71eV. Further the co-adsorption of both reactants on $Au_2Cl_6/GRN-I$ was investigated. After geometry optimization, both adsorbed reactants are activated on $Au_2Cl_6/GRN-I$,

with the $E_{\text{ads}}(\text{co-adsorption})$ of 1.58 eV. It is indicated that the N-doped support of GRN-I can stabilize the gold species Au_2Cl_6 and enhance the interaction between Au_2Cl_6 and HCl, which can inhibit the lost of Cl atoms from Au_2Cl_6 and retard the reduction of Au^{3+} and then increase the long-term stability of Au-based catalysts. This work provides a useful guidance on improving the long-term stability of Au-catalysts for acetylene hydrochlorination via the N-doped carbon support.

Acknowledgment

We gratefully acknowledge the support for this work by the Special Funds for Major State Research Program of China (2012CB720300), 863(2012AA062901), NSFC (21176174), and Program for Changjiang Scholars and Innovative Research Team in University (IRT1161).

Reference

1. J. Wilcox, E. Rupp, S. C. Ying, D. H. Lim, A. S. Negreira, A. Kirchofer, F. Feng and K. Lee, *Int. J. Coal Geol.*, 2012, **90**, 4-20.
2. E. Sasmaz, S. Aboud and J. Wilcox, *J. Phys. Chem. C*, 2009, **113**, 7813-7820.
3. G. Hutchings, *Journal of Catalysis*, 1985, **96**, 292-295.
4. M. Conte, C. J. Davies, D. J. Morgan, T. E. Davies, A. F. Carley, P. Johnston and G. J. Hutchings, *Catal. Sci. Technol.*, 2013, **3**, 128-134.
5. M. Conte, C. J. Davies, D. J. Morgan, T. E. Davies, D. J. Elias, A. F. Carley, P. Johnston and G. J. Hutchings, *Journal of Catalysis*, 2013, **297**, 128-136.
6. H. Zhang, B. Dai, X. Wang, W. Li, Y. Han, J. Gu and J. Zhang, *Green Chemistry*, 2013, **15**, 829-836.
7. H. Zhang, B. Dai, X. Wang, L. Xu and M. Zhu, *J. Ind. Eng. Chem.*, 2012, **18**, 49-54.
8. B. Nkosi, M. D. Adams, N. J. Coville and G. J. Hutchings, *Journal of Catalysis*, 1991, **128**, 378-386.
9. J. L. Zhang, W. Sheng, C. L. Guo and W. Li, *RSC Advances*, 2013, **3**, 21062-21068.
10. S. J. Wang, B. X. Shen and Q. L. Song, *Catal Lett*, 2010, **134**, 102-109.
11. M. Conte, A. F. Carley, G. Attard, A. A. Herzing, C. J. Kiely and G. J. Hutchings, *Journal of Catalysis*, 2008, **257**, 190-198.
12. H. Y. Zhang, B. Dai, X. G. Wang, L. L. Xu and M. Y. Zhu, *J. Ind. Eng. Chem.*, 2012, **18**, 49-54.
13. H. Zhang, B. Dai, W. Li, X. Wang, J. Zhang, M. Zhu and J. Gu, *Journal of Catalysis*, 2014, **316**, 141-148.
14. B. Wang, L. Yu, J. Zhang, Y. Pu, H. Zhang and W. Li, *RSC Advances*, 2014, **4**, 15877-15885.
15. X. Li, M. Zhu and B. Dai, *Applied Catalysis B: Environmental*, 2013, **142-143**, 234-240.

16. C. C. Huang, C. Li and G. Q. Shi, *Energy Environ. Sci.*, 2012, **5**, 8848-8868.
17. D. W. Boukhvalov and Y. W. Son, *Nanoscale*, 2012, **4**, 417-420.
18. Y. Li, Y. Zhao, H. Cheng, Y. Hu, G. Shi, L. Dai and L. Qu, *J. Am. Chem. Soc.*, 2011, **134**, 15-18.
19. H. Wang, T. Maiyalagan and X. Wang, *ACS Catalysis*, 2012, **2**, 781-794.
20. K. Parvez, S. Yang, Y. Hernandez, A. Winter, A. Turchanin, X. Feng and K. Müllen, *ACS Nano*, 2012, **6**, 9541-9550.
21. C. He, J. J. Zhang and P. K. Shen, *Journal of Materials Chemistry A*, 2014, **2**, 3231-3236.
22. J. Liang, X. Du, C. Gibson, X. W. Du and S. Z. Qiao, *Adv. Mater.*, 2013, **25**, 6226-6231.
23. X. Zhong, H. Yu, G. Zhuang, Q. Li, X. Wang, Y. Zhu, L. Liu, X. Li, M. Dong and J.-g. Wang, *Journal of Materials Chemistry A*, 2014, **2**, 897-901.
24. P. Wu, P. Du, H. Zhang and C. Cai, *Phys. Chem. Chem. Phys.*, 2013, **15**, 6920-6928.
25. A. B. Ayusheev, O. P. Taran, I. A. Seryak, O. Y. Podyacheva, C. Descorme, M. Besson, L. S. Kibis, A. I. Boronin, A. I. Romanenko, Z. R. Ismagilov and V. Parmon, *Appl. Catal. B-Environ.*, 2014, **146**, 177-185.
26. M. N. Groves, C. Malardier-Jugroot and M. Jugroot, *J. Phys. Chem. C*, 2012, **116**, 10548-10556.
27. L. P. Zhang, J. B. Niu, L. Dai and Z. H. Xia, *Langmuir*, 2012, **28**, 7542-7550.
28. L. P. Zhang and Z. H. Xia, *J. Phys. Chem. C*, 2011, **115**, 11170-11176.
29. J. Akola and H. Häkkinen, *Physical Review B*, 2006, **74**, 165404.
30. J. Zhang, Z. He, W. Li and Y. Han, *RSC Advances*, 2012, **2**, 4814-4821.
31. M. Conte, C. J. Davies, D. J. Morgan, A. F. Carley, P. Johnston and G. J. Hutchings, *Catal Lett*, 2014, **144**, 1-8.
32. B. Hammer, L. B. Hansen and J. K. Nørskov, *Physical Review B*, 1999, **59**, 7413-7421.
33. A. Srivastava, A. Jain, R. Kurchania and N. Tyagi, *J. Comput. Theor. Nanosci.*, 2012, **9**, 1008-1013.

34. E. C. Anota and G. H. Coccoletzi, *Physica E* 2014, **56**, 134–140
35. K. Sun, Minhua Zhang, Lichang Wang, *Chemical Physics Letters* 2013, **585**, 89–94
36. T. C. Dinadayalane and J. Leszczynski, *Struct Chem*, 2010, **21**, 1155-1169.
37. S. Furlan and P. Giannozzi, *Phys. Chem. Chem. Phys.*, 2013, **15**, 15896-15904.
38. D. Geng, Y. Chen, Y. Chen, Y. Li, R. Li, X. Sun, S. Ye and S. Knights, *Energy Environ. Sci.*, 2011, **4**, 760-764.
39. R. Varns and P. Strange, *J. Phys.-Condes. Matter*, 2008, **20**, 225005-225012.
40. A. Martin, S. Biplab, E. Olle and V. S. Natalia, *Journal of Physics: Condensed Matter*, 2011, **23**, 205301.
41. O. Üzengi Aktürk and M. Tomak, *Physical Review B*, 2009, **80**, 085417.
42. Wikipedia, [http://en.wikipedia.org/wiki/Gold\(I\)_chloride](http://en.wikipedia.org/wiki/Gold(I)_chloride), (accessed June, 2014)
43. K. A. Ritter and J. W. Lyding, *Nat Mater*, 2009, **8**, 235-242.
44. K. K. Paulla, A. J. Hassan, C. R. Knick and A. A. Farajian, *RSC Advances*, 2014, **4**, 2346-2354.

Table 1. Charge distribution of Au₂Cl₂ adsorbed on different supports

Atom number	Au ₂ Cl ₂	GR	GRN-I	GRN-II	GRN-III
Cl 1	-0.236	-0.308	-0.334	-0.309	-0.279
Cl 2	-0.124	-0.202	-0.268	-0.209	-0.278
Cl1+Cl2	-0.36	-0.51	-0.602	-0.518	-0.557
Au 1	0.102	0.049	0.034	0.022	0.046
Au 2	0.258	0.103	0.005	0.091	0.024
Au1+Au2	0.360	0.152	0.039	0.113	0.070
Net charge	0	-0.358	-0.563	-0.405	-0.487

Table 2. Charge distribution of Au₂Cl₆ adsorbed on different supports

Atom number	Au ₂ Cl ₆	GR	GRN-I	GRN-II	GRN-III
Au 1	0.132	0.130	0.119	0.128	0.130
Au 2	0.132	0.135	0.151	0.145	0.129
Cl1	-0.102	-0.213	-0.217	-0.210	-0.231
Cl2	0.072	-0.009	-0.033	-0.017	-0.036
Cl3	-0.102	-0.217	-0.276	-0.240	-0.252
Cl4	-0.102	-0.214	-0.226	-0.213	-0.233
Cl5	0.072	-0.011	-0.075	-0.035	-0.040
Cl6	-0.102	-0.227	-0.331	-0.271	-0.261
Total charge of two Au atoms	0.264	0.265	0.270	0.273	0.259
Total charge of six Cl atoms	-0.264	-0.891	-1.158	-0.986	-1.053
Au2-Cl6 bond order ^a	0.505	0.471	0.415	0.450	0.459
Net charge ^b	0	-0.626	-0.888	-0.713	-0.794

^a: Au1 and Au2 indicate the first and the second Au atoms, while Cl1 to Cl6 is respectively the first to the sixth chlorine atom in Au₂Cl₆ complex. The bond between the second Au atom and the sixth chlorine atom is denoted as Au2-Cl6.

^b: Net charge is the summation of the charge on every atom from Au₂Cl₆.

Captions for Figures

Figure 1. Three typical structures of N-doped graphene. Color code: C, grey; H, white; N, blue.

Figure 2. The Mulliken charge (a~d) and the bond length (Å, a'~d') of different supports, including (a, a') GR, (b, b') GRN-I, (c, c') GRN-II and (d, d') GRN-III.

Figure 3. Adsorption structure of Au atom on the support of (a) GR, (b) GRN-I, (c) GRN-II and (d) GRN-III, with some bond length (Å) labeled in red. Atom color code: C, grey; H, white; N, blue; Au, yellow.

Figure 4. Deformation electron density of Au atom adsorbed on different supports of (a) GR, (b) GRN-I, (c) GRN-II and (d) GRN-III. The purple (gaining electron) and the cyan (losing electron) surfaces correspond to opposite electron spins with a value of 0.03 electrons/Å³. Atom color code: N, blue; Au, yellow.

Figure 5. Adsorption structure of Au dimer on the support of (a) GR, (b) GRN-I, (c) GRN-II and (d) GRN-III, with some bond length (Å) labeled in red. Atom color code: C, grey; H, white; N, blue; Au, yellow.

Figure 6. The top panel shows two optimized structures for Au₂Cl₂, involving the triangular (I) and the tetragonal model (II). The bottom panel shows the adsorption structure of Au₂Cl₂, adopting the triangular model on the support of (a) GR, (b) GRN-I, (c) GRN-II and (d) GRN-III. Atoms Cl and Au are respectively numbered in light green and yellow, with some bond length (Å) labeled in red. Atom color code: C, grey; H, white; N, blue; Au, yellow; Cl, green.

Figure 7. Adsorption structure and the related bond length (\AA) of Au_2Cl_6 on the support of (a) GR, (b) GRN-I, (c) GRN-II and (d) GRN-III. Atom color code: C, grey; H, white; N, blue; Au, yellow; Cl, green.

Figure 8. PDOS of Au_2Cl_6 . Atoms of Au2, Cl6 and H after adsorption and H atom before adsorption are arranged from top to bottom on (a) GRN-I (b) GR

Figure 9. The adsorption energy of Au dimer, Au_2Cl_2 and Au_2Cl_6 on four different supports.

Figure 10. The transferred charge (Δq) from different support to Au dimer, Au_2Cl_2 and Au_2Cl_6 .

Figure 11. Optimized structures of HCl adsorbed on Au_2Cl_6 with the support of (a) GR, (b) GRN-I, (c) GRN-II and (d) GRN-III. Atom color code: C, grey; H, white; N, blue; Au, yellow; Cl, green.

Figure 12. Adsorption structure of C_2H_2 on Au_2Cl_6 with the support of (a) GR, (b) GRN-I, (c) GRN-II and (d) GRN-III. Atom color code: C, grey; H, white; N, blue; Au, yellow; Cl, green.

Figure 13. The optimized configuration of co-adsorbed C_2H_2 and HCl on Au_2Cl_6 with the GRN-I. Atom color code: C, grey; H, white; N, blue; Au, yellow; Cl, green.

Figure 1.

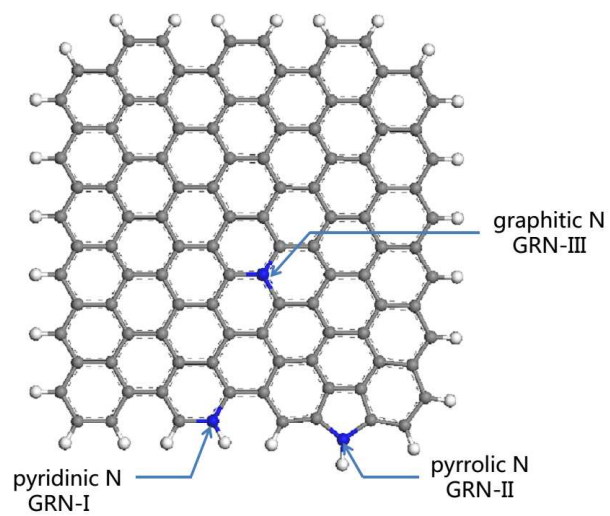


Figure 2.

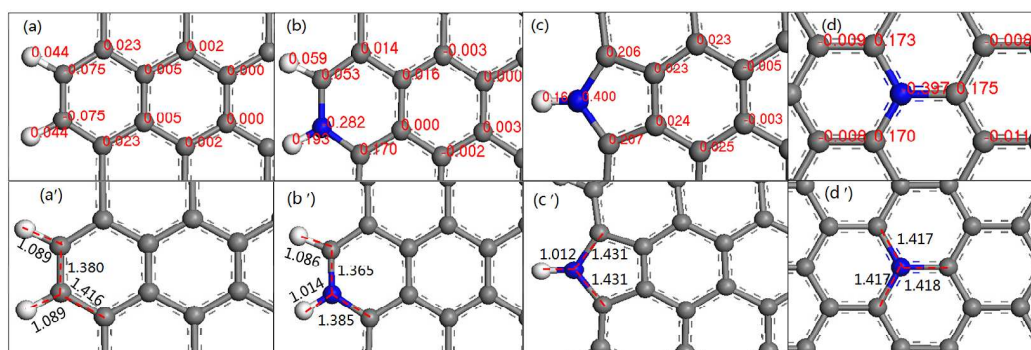


Figure 3.

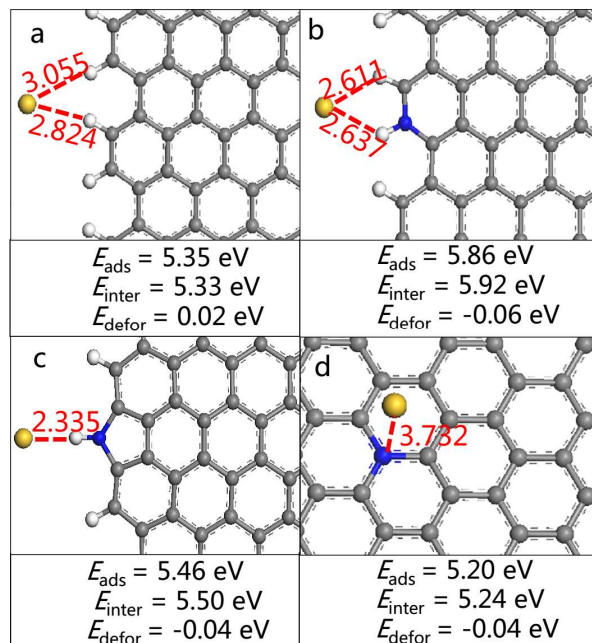


Figure 4.

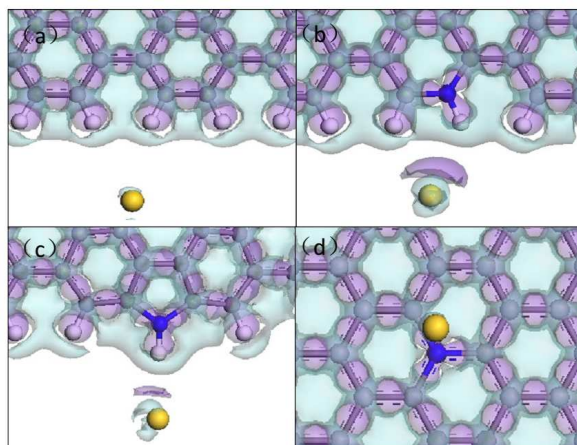


Figure 5.

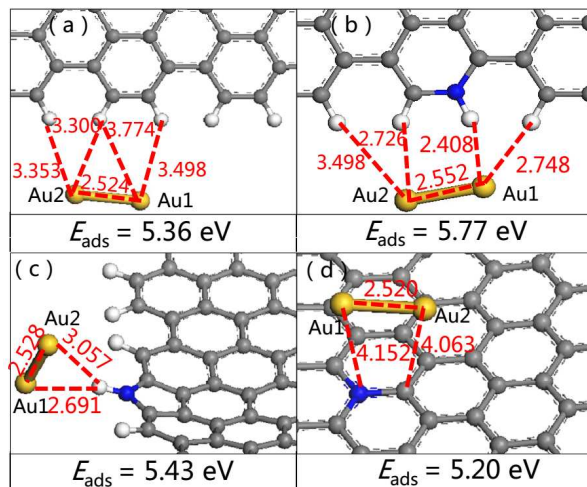


Figure 6.

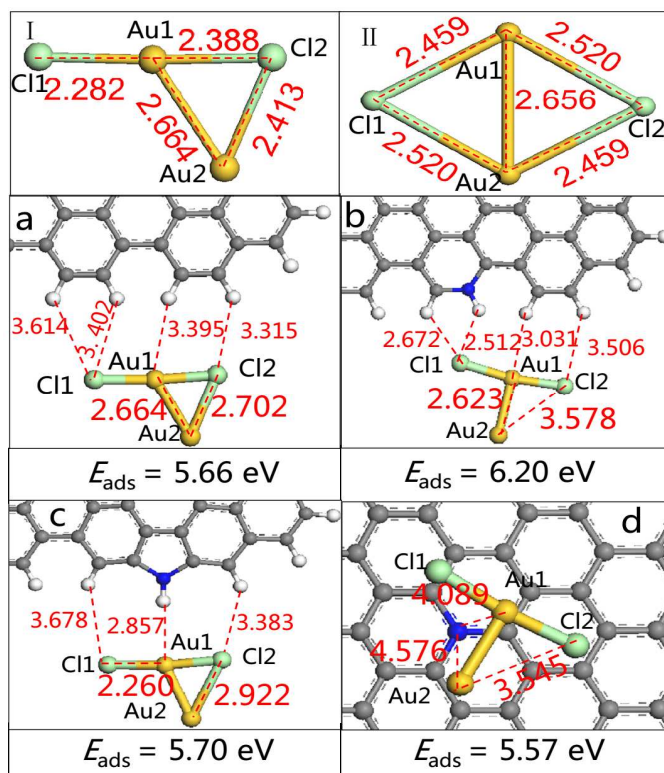


Figure 7.

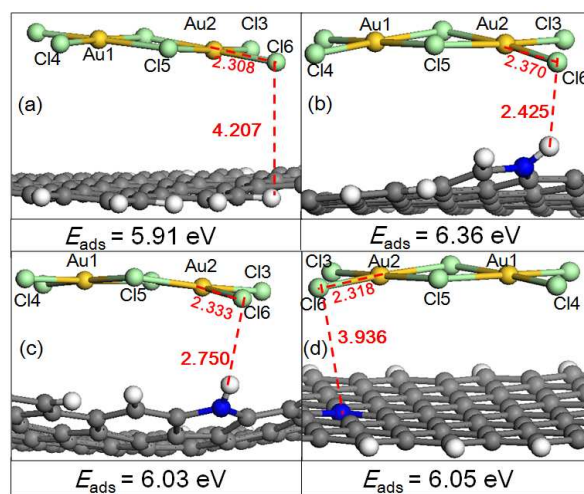


Figure 8.

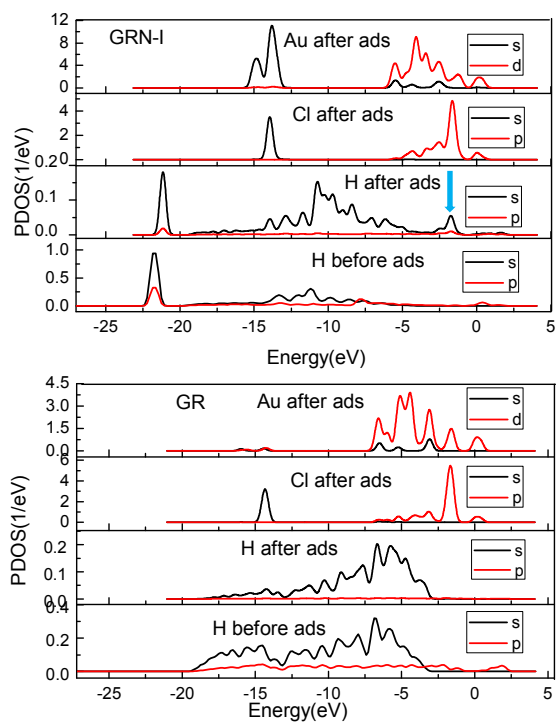


Figure 9.

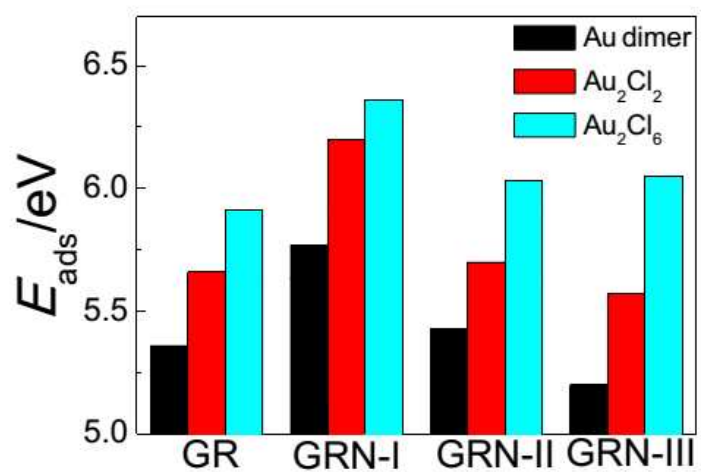


Figure 10

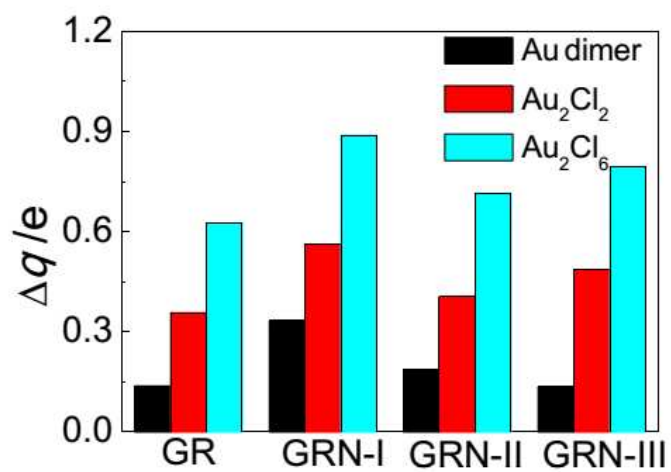


Figure 11.

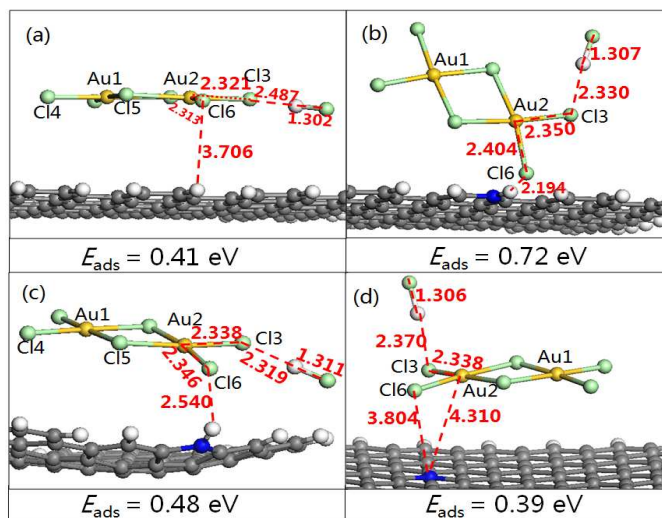


Figure 12.

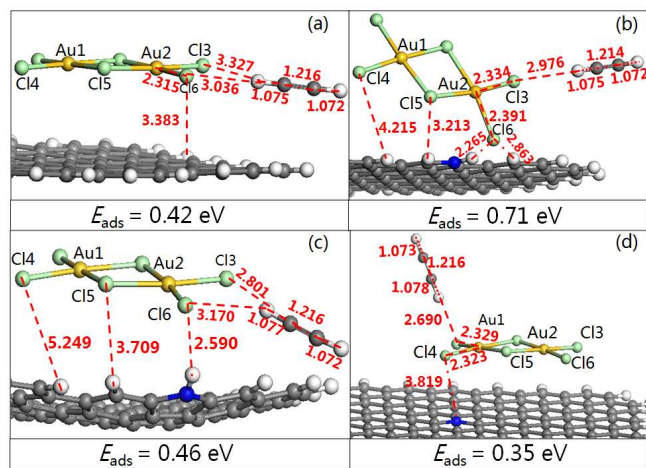


Figure 13.

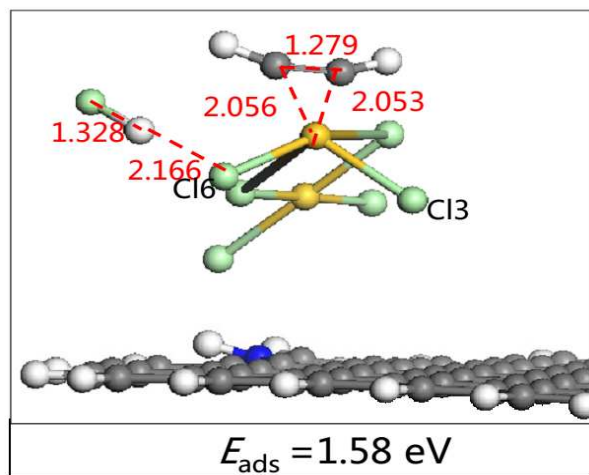
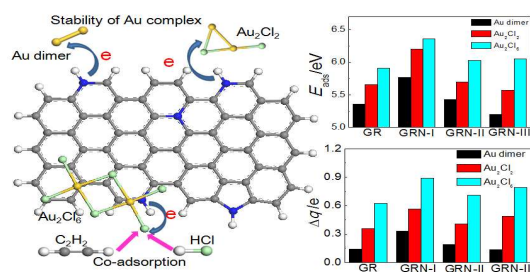


Table of contents entry



The stabilities of gold species on N-doped graphene increase with its valence state. Au₂Cl₆ interacts preferentially with HCl on N-doped supports, enhancing the stability of Au catalysts for acetylene hydrochlorination.